Separation Science and Technology
Publication details, including instructions for authors and subscription information:
http://www.informaworld.com/smpp/title~content=t713708471

Line Shapes in Gas Chromatography. III. Solute-Solute Interactions in Preparative Columns

David J. Wilson[a]
[a] Department of Chemistry, Vanderbilt University, Nashville, Tennessee

To cite this Article Wilson, David J.(1987) 'Line Shapes in Gas Chromatography. III. Solute-Solute Interactions in Preparative Columns', Separation Science and Technology, 22: 8, 1835 — 1849
To link to this Article: DOI: 10.1080/01496398708057615
URL: http://dx.doi.org/10.1080/01496398708057615

SEPARATION SCIENCE AND TECHNOLOGY, 22(8-10), pp. 1835-1849, 1987

Line Shapes in Gas Chromatography. III. Solute-Solute Interactions in Preparative Columns

---

DAVID J. WILSON

DEPARTMENT OF CHEMISTRY
VANDERBILT UNIVERSITY
NASHVILLE, TENNESSEE 37235

Abstract

The effects of solute-solute interactions on the shapes of the bands in preparative gas chromatography are modeled by numerical integration of the coupled sets of differential equations describing solute movement. An asymmetrical upwind algorithm is used to describe advection; this greatly reduces the numerical dispersion which is inherent in the theoretical plate method. A microcomputer was used for doing the computations.

INTRODUCTION

The calculation of band shapes is of particular importance in preparative gas chromatography, where column packings with high liquid loadings and the use of large sample sizes frequently result in behavior which is strongly nonideal. Most of the relevant literature on the calculation of band shapes was reviewed in an earlier paper (*1*), to which the reader is referred.

The method of attack which shall be followed here is the numerical integration of the differential equations describing the movements of solutes in the gas chromatography column. Vink's mesh technique for solving the differential equations (*2*, *3*) is similar. Houghton used a perturbation approach to include the effects of diffusion and nonequilibrium mass transport (*4*). Giddings's stochastic method (*5*) for doing line shape calculations should also lend itself to handling the problem of solute-solute interactions which is addressed here. In an earlier paper Giddings (*6*) discussed the relationships between the theoretical plate model and the two "rate" theories—the stochastic theory and the concentration of material theory.

One of the most powerful and flexible attacks on the band shape problem has been given by Guiochon and his coworkers (*7*). Their model is based on the solution of the appropriate partial differential equation, and permits them to include both the influence of the isotherm curvature at zero concentration and the perturbation of the flow rate due to solute exchange between the mobile and stationery phases. Peak area, axial dispersion coefficient, limit retention time, and leaning coefficient are the experimental parameters needed to use the model. The model takes kinetic effects into account by means of a global dispersion factor, and neglects adsorption-desorption kinetics. It is good for low to moderate column loadings.

In two recent papers (*1*, *8*) we utilized so-called asymmetrical upwind algorithms for modeling the advection term in the partial differential equation describing the movement of a single solute through a gas chromatographic column. Leonard (*9*, *10*) has used such algorithms and showed that they result in greatly reduced numerical dispersion. We have found them to be very useful in modeling the flow of contaminants in groundwater (*11*, *12*) and in modeling the operation of ion-exchange columns (*13*, *14*). In the modeling of column separations, a very large number of theoretical transfer units is required if the column is reasonably efficient. As discussed in an earlier paper (*8*), this presents severe problems to the numerical analyst.

In preparative column work, sample sizes are made as large as possible; therefore, if solute-solute interactions occur, they are likely to be particularly significant in preparative columns. Interactions may be of a number of types, such as 1) the presence of Compound B may enhance the solubility of Compound A in the stationary phase, 2) the presence of Compound B may reduce the solubility of Compound A in the stationary phase, and 3) there may actually be some sort of association complex formed between the two compounds. An example of this last would be the chromatographing of a mixture of a moderately acidic phenol (say 2,4,5-trichlorophenol) with an organic base such as benzylamine. Such interactions would certainly change retention times from the values which would be obtained with samples containing only one of the two solutes, and we might expect that band shapes may be severely distorted, perhaps to the point where chromatographic resolution of the mixture under the given conditions of temperature and loading becomes impossible.

In the following sections we examine the effects of compound formation and solubility modification by use of mathematical models.

Such calculations may be of use in interpreting data and also in designing separations. For example, interfering interactions can obviously be reduced by decreasing sample sizes. If the parameters in the theory can be estimated, it then becomes possible to determine by simulation the maximum sample size which still provides adequate resolution of the mixture. We first present and analyze the models. Results are then presented as graphs showing the effects predicted by the models. Finally, some general conclusions are drawn from the results, and some future work in the area is suggested.

ANALYSIS

Figure 1 illustrates our model for the operation of a gas chromatographic column. As before (*8*), we start out by developing a local equilibrium theoretical plate model. This is then modified by replacing the theoretical plate advection terms by one of the asymmetrical upwind

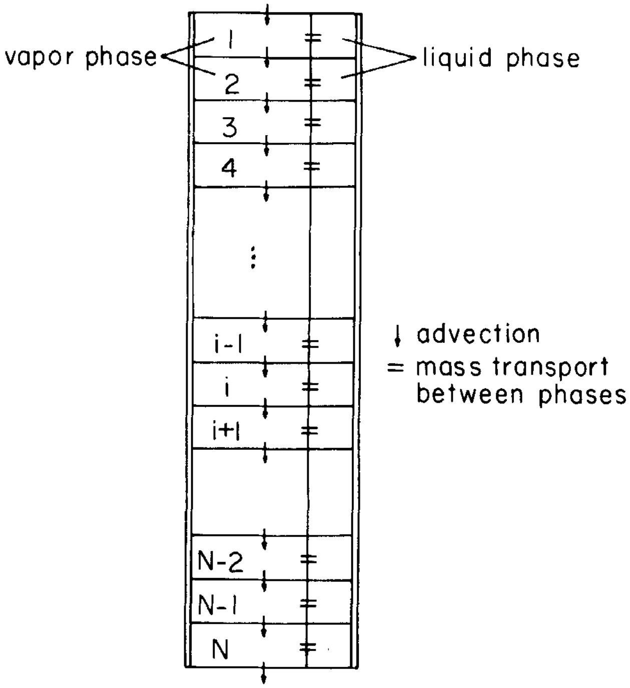

FIG. 1. The model used to describe column operation.

algorithms tested previously (*1*, *8*) and found to markedly reduce numerical dispersion. The coupling between the differential equations describing the movement of the two solutes through the column depends on the nature of the interaction between the solutes. We examine the coupling due to compound formation and that due to linear dependence of the Henry's law constant K_A on the concentration of Solute B. We assume that both solutes obey Henry's law; the use of more complex isotherms (such as the Langmuir isotherm) presents no difficulties.

The column is partitioned into N compartments each of length Δx and radius r (cm). Let the volumetric flow rate of the carrier gas be υ mL/s; let the voids fraction of the column be υ_g and the volume fraction of the liquid phase in the column be υ_l. The movements of the two solutes in the column are then described by

$$\frac{dm_i^a}{dt} = \upsilon(c_{g,i-1} - c_{g,i}^a) \tag{1}$$

$$\frac{dm_i^b}{dt} = \upsilon(c_{g,i-1}^b - c_{g,i}^b) \tag{2}$$

The solutes are assumed to obey Henry's law which yields

$$c_{l,i}^a = K^a c_{g,i}^a \tag{3}$$

$$c_{l,i}^b = K^b c_{g,i}^b \tag{4}$$

Here m_i^a = moles of Solute A in Compartment i
$c_{g,i}^a$ = concentration of Solute A in the vapor phase in Compartment i, mol/mL
$c_{l,i}^a$ = concentration of Solute A in the liquid phase in Compartment i, mol/mL
K^a = Henry's law constant for Solute A, dimensionless
Superscripts b denote corresponding quantities for Solute B.

We assume that A and B can form an association complex AB which is essentially nonvolatile under the column operating conditions. Then

$$K^{ab} = \frac{c_{l,i}^{ab}}{c_{l,i}^a \cdot c_{l,i}^b} \tag{5}$$

where $c_{l,i}^{ab}$ is the concentration of the complex in the liquid phase of Compartment i. Mass balances for A and B in Compartment i give

$$m_i^a = V_l(c_{l,i}^a + c_{l,i}^{ab}) + V_g c_{gi}^a \tag{6}$$

$$m_i^b = V_l(c_{l,i}^b + c_{l,i}^{ab}) + V_g c_{gi}^b \tag{7}$$

where

$$V_l = \pi r^2 \Delta x v_l \tag{8}$$

$$V_g = \pi r^2 \Delta x v_g \tag{9}$$

From Eqs. (1) and (2) we calculate the changes in the mole numbers m_i^a and m_i^b with time. It is then necessary to calculate the values of the concentrations in terms of the mole numbers. This is done as follows. Combining Eqs. (3), (4), and (5) yields

$$c_{l,i}^{ab} = K^a K^b K^{ab} c_{g,i}^a c_{g,i}^b \tag{10}$$

Substitution of Eqs. (3) and (10) in Eq. (6) gives, after rearrangement,

$$c^a = \frac{m_i^a}{V_l K^a(1 + K^{ab} K^b c_{g,i}^b) + V_g} \tag{11}$$

In similar fashion,

$$c_{g,i}^b = \frac{m_i^b}{V_l K^b(1 + K^{ab} K^a c_{g,i}^a) + V_g} \tag{12}$$

It is possible to substitute Eq. (11) into Eq. (12) and obtain a quadratic equation in $c_{g,i}^b$ alone, but iterative solution of these two equations is very fast and easier to program.

Equations (1) and (2), denoted as Algorithm 1, yield a great deal of numerical dispersion. We had previously found that linear combinations of Algorithm 1 with a more elaborate asymmetrical upwind algorithm yields low numerical dispersion and high stability. Here we use as Algorithm 2 the formula

$$\frac{dm_i^a}{dt} = v\left(-\frac{1}{8}c_{g,i-2}^a + \frac{7}{8}c_{g,i-1}^a - \frac{3}{8}c_{g,i}^a - \frac{3}{8}c_{g,i+1}^a\right) \tag{13}$$

Then in place of Eq. (1) we use

$$dm_i^a/dt = b \cdot (\text{Algorithm 2}) + (1 - b) \cdot (\text{Algorithm 1}) \tag{14}$$

where $0 < b < 1$. Dispersion of the bands can be controlled by the choice of b; the smaller b, the broader the band.

The solute-solute interactions could involve changes in the values of the Henry's law constants. We examine the following model

$$K^a = K_0^a(1 + K^{ab}c_l^b) \tag{15}$$

$$K^b = K_0^b(1 + K^{ba}c_l^a) \tag{16}$$

where K^{ab} and K^{ba} may be positive or negative. The concentrations in the liquid phases then satisfy the equations

$$c_l^a = K_0^a(1 + K^{ab}c_l^b)c_g^a \tag{17}$$

$$c_l^b = K_0^b(1 + K^{ba}c_l^a)c_g^b \tag{18}$$

A mass balance on Solute A in Compartment i gives

$$m_i^a = V_lc_{l,i}^a + V_gc_{g,i}^a \tag{19}$$

$$= [V_lK_0^a(1 + K^{ab}c_{l,i}^b) + V_g]c_{g,i}^a \tag{20}$$

from which we obtain

$$c_{g,i}^a = \frac{m_i^a}{V_lK_0^a(1 + K^{ab}c_{l,i}^b) + V_g} \tag{21}$$

In similar fashion a mass balance on Solute B yields

$$c_{g,i}^b = \frac{m_i^b}{V_lK_0^b(1 + K^{ba}c_{l,i}^a) + V_g} \tag{22}$$

For given values of m_i^a and m_i^b, Eqs. (21), (22), (17), and (18) are solved iteratively to obtain $c_{g,i}^a$, $c_{g,i}^b$, $c_{l,i}^a$, and $c_{l,i}^b$.

The remainder of the band shape calculations (the integration of the differential equations) follows exactly as before. A two-step predictor-corrector method described by Ralston and Wilf (*15*) was used. An outline of the method is as follows:

Starter: $$y^*(\Delta t) = y(0) + \frac{dy}{dt}(0)\Delta t \tag{23}$$

$$\text{Predictor:} \qquad y^*(t + \Delta t) = y(t - \Delta t) + \frac{dy}{dt}(t)2\Delta t \tag{24}$$

$$\text{Corrector:} \quad y(t + \Delta t) = y(t) + \left[\frac{dy^*}{dt}(t + \Delta t) + \frac{dy}{dt}(t)\right]\frac{\Delta t}{2} \tag{25}$$

RESULTS

Programs implementing the two models (solute–solute association and solute-dependent Henry's law constants) were written for a Zenith 150 computer and compiled. Representative parameters are listed in Table 1; these parameters were used in making the run plotted in Fig. 2. This run required 17 min of computer time on a machine with an Intel 8088 microprocessor with a 4.77 MHz clock. The run shown in Fig. 2 includes no solute–solute interactions, so the band shapes in this figure are ideal. These bands can be narrowed by increasing the value of N and/or increasing the value of b, the parameter which determines the relative proportions of the upwind asymmetrical algorithm and the theoretical plate algorithm used to represent advection. The two peaks are completely resolved, with retention times $t_A = 375$ s and $t_B = 219$ s, and widths at half-height $w_A = 73$ s and $w_B = 43$ s.

Figures 3 and 4 show the effects on band shapes of the formation of an AB association complex. In Fig. 3, K^{ab} is given a value of 10^6 mL/mol; in Fig. 4 the value of this parameter is 5×10^6 mL/mol. The effects of association on the peaks are substantial in Fig. 3 and disastrous in Fig. 4. In Fig. 3 the retention times are $t_A = 425$ s and $t_B = 230$ s, markedly larger than the retention times found in Fig. 2. Also, the B peak is much broader and has a pronounced trailing tail which overlaps with the A peak. In Fig. 4 the A peak shows very severe leading tailing and a retention time of

TABLE 1
Representative Parameter Values

Column length = 200 cm	$K^a = 50$
$N = 50$	$K^b = 25$
$b = 0.7$	$K^{ab} = 0$
Column diameter = 2 cm	Moles of A in sample = 1×10^{-6}
$v_l = 0.01$	Moles of B in sample = 1×10^{-6}
$v_g = 0.1$	$dt = 1.0$ s
$v = 1.0$ mL/s	

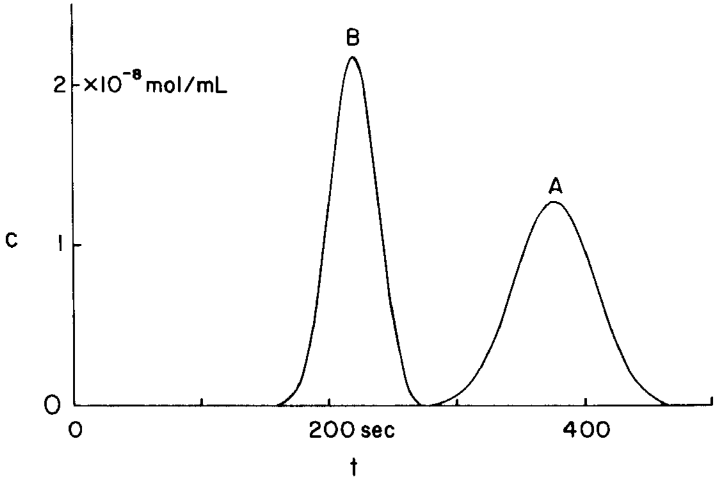

FIG. 2. Reference band shapes. There are no solute-solute interactions in the run plotted here. Parameters are given in Table 1.

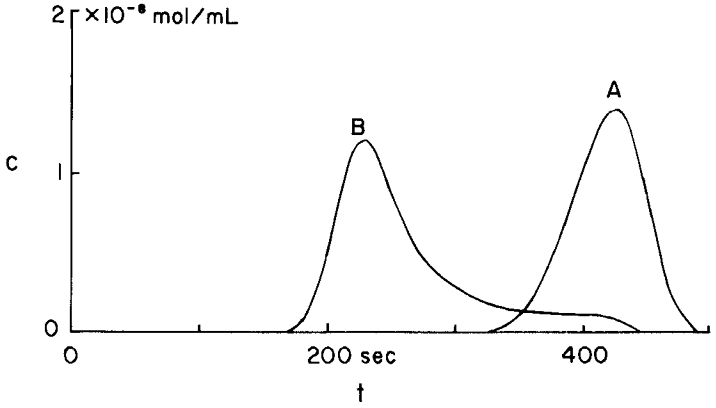

FIG. 3. Effect of A-B association on band shapes. Parameters are given in Table 1 except that a value of 10^6 mL/mol was used for the equilibrium constant of the reaction A + B = AB, K^{ab}.

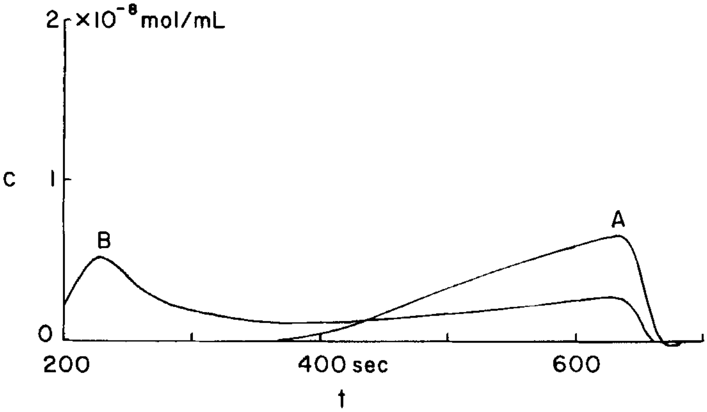

FIG. 4. Effect of A-B association on band shapes. Parameters are given in Table 1 except that $K^{ab} = 5 \times 10^6$ mL/mol.

about 630 s. The B band in Fig. 4 shows a bizarre bimodal distribution with maxima at 228 and 625 s. The resolution of the two compounds in Fig. 4 is obviously unsatisfactory.

The run plotted in Fig. 5 has parameters identical to those used in the run shown in Fig. 4 except that the sample size is one-tenth as large. The form of the equilibrium expression for complex formation, Eq. (5) shows that decreasing the sample size should shift the equilibrium from AB complex toward isolated A and B. A comparison of Figs. 4 and 5 indicates that this is indeed the case. The retention times in Fig. 5 are $t_A = 390$ s and $t_B = 227$ s, only slightly larger than those found in Fig. 2, the ideal case. Also, resolution of the bands in Fig. 5 is virtually complete.

The effects of increasing N, the number of compartments used to represent the column, is seen by comparing Fig. 2, for which $N = 50$, and Fig. 6, for which $N = 100$. (Note the change in scale of the ordinates.) Increasing N from 50 to 100 causes a decrease in w_A from 73 to 53 s, and a decrease in w_B from 43 to 29 s. As one would expect, the line widths are approximately in the ratio of $\sqrt{100/50}$ (1.38 and 1.48).

A comparison of Figs. 2 ($b = 0.7$) and 7 ($b = 0.9$) shows the effect of varying the proportions of the asymmetrical upwind algorithm and the theoretical plate algorithm. Instability is just beginning to be seen in Fig. 7—note the small dips on the trailing sides of the bands. The retention times are virtually unaffected. The half-widths for the peaks in Figs. 2 and 7 are $w_A = 73$ and 55 s, and $w_B = 43$ and 32.5 s; evidently increasing the contribution of the asymmetrical upwind algorithm results

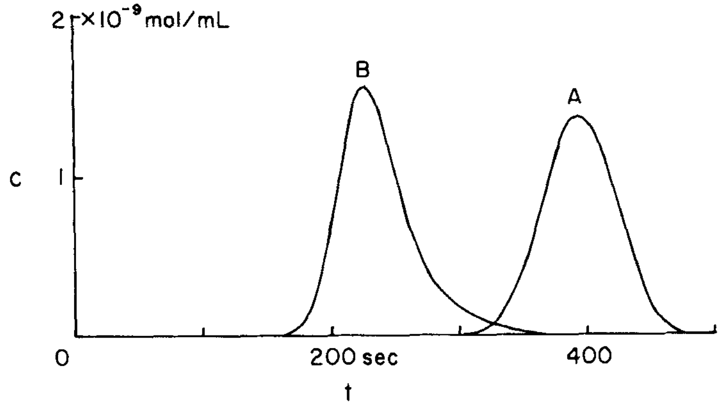

FIG. 5. Effect of a decrease in sample size when chromatographing an associating mixture. Parameters are given in Table 1 except that $K^{ab} = 5 \times 10^6$ mL/mol, $m_a = 10^{-7}$, $m_b = 10^{-7}$ mol.

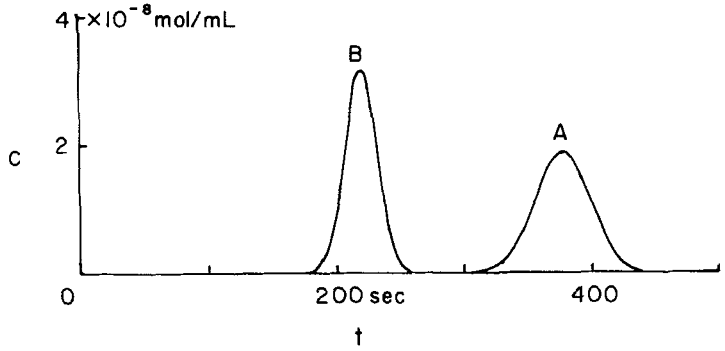

FIG. 6. Effect of the number of compartments used to represent the column on band shapes. Parameters are given in Table 1 except that $N = 100$ instead of 50, and $dt = 0.5$ s instead of 1.0 s.

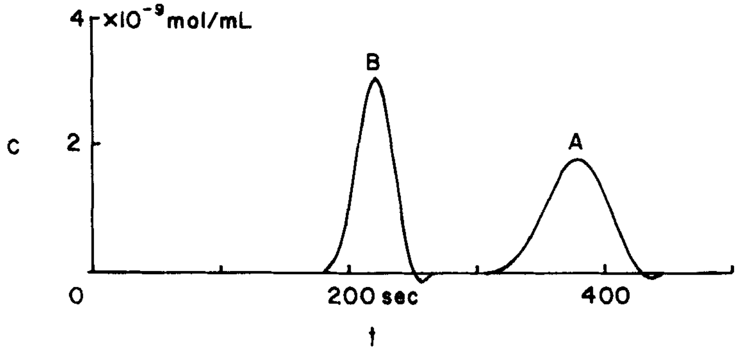

FIG. 7. Effect of the parameter *b* on the band shapes. Parameters are given in Table 1 except that *b* (see Eq. 14) = 0.9 instead of 0.7. Note the narrowing of the bands.

in narrower bands. Increasing *b* above 0.9 results in undesirable instabilities, as indicated by increased oscillatory behavior.

Figures 8, 9, 10, and 11 show some of the effects resulting from concentration-dependent Henry's law constants as exemplified by Eqs. (15) and (16).

In Fig. 8, in which both interaction constants K^{ab} and K^{ba} are 1×10^6 mL/mol, the leading peak (B) is very markedly broadened and shows a trailing tail which would interfere with resolution of the two compounds. The retention times are $t_A = 455$ s and $t_B = 235$ s, significantly increased over the values of 375 and 219 s for the ideal case.

The Henry's law interaction constants used in the run plotted in Fig. 9 are $K^{ab} = 10^6$ mL/mol, $K^{ba} = 0$. The appearances of the bands in this run are virtually identical to those in the ideal case (Fig. 2). The retention times are $t_A = 390$, as compared to 375 s for the ideal case; and $t_B = 218$, compared to 219 s for the ideal case. Aside from a slight increase in t_A, the interaction used in this run has had essentially no effect.

The Henry's law interaction constants used in Fig. 10 are $K^{ab} = 0$, $K^{ba} = 10^6$ mL/mol. Unlike the run in Fig. 9, here the effects of the Henry's law concentration dependence are very large and totally destructive of resolution. The B peak shows extensive leading tailing, and the two peaks overlap nearly completely. The retention times are $t_A = 375$ s (unchanged from Fig. 2) and $t_B = 365$ s (compared to 219 s in Fig. 2).

In Fig. 11 the Henry's law interaction constants are $K^{ab} = 0$, $K^{ba} = 3 \times 10^6$ mL/mol. The resulting bands show some quite unusual features. The retention times are $t_A = 375$ s and $t_B = 413$ s (compared to 219 s in Fig. 2). The interaction has trapped Solute B behind the plug of Solute A

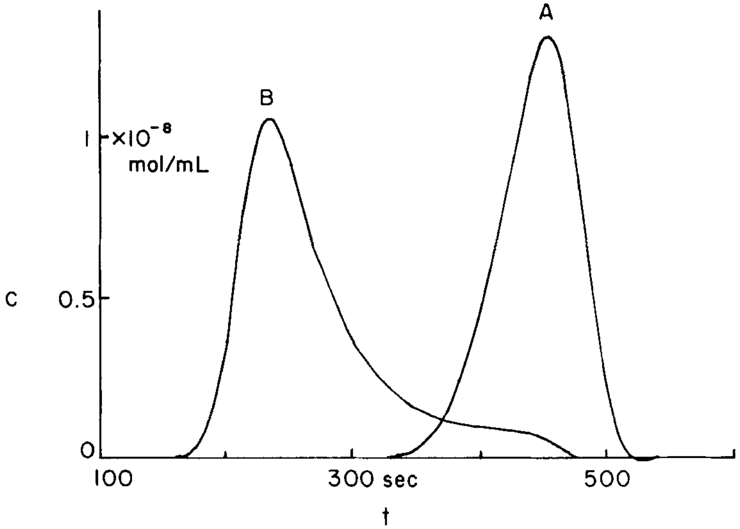

FIG. 8. Effect of concentration-dependent Henry's law constants on band shape. Parameters are given in Table 1 except that K^{ab} and K^{ba} in Eqs. (15) and (16) are given by 10^6 mL/mol instead of zero.

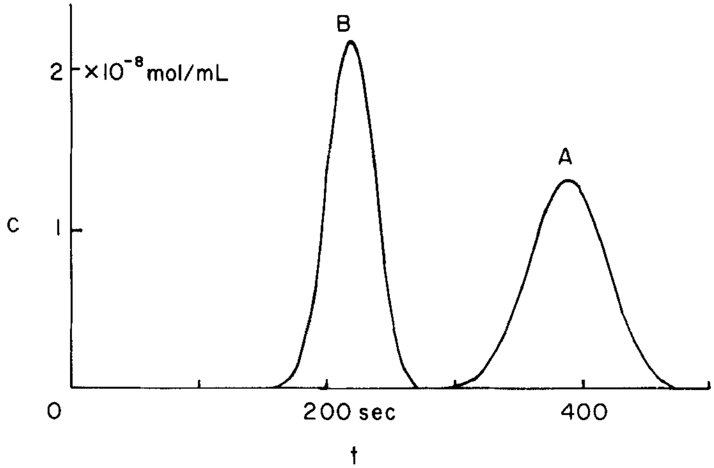

FIG. 9. Effect of concentration-dependent Henry's law constants on band shape. Parameters are given in Table 1 except that $K^{ab} = 10^6$ mL/mol ($K^{ba} = 0$).

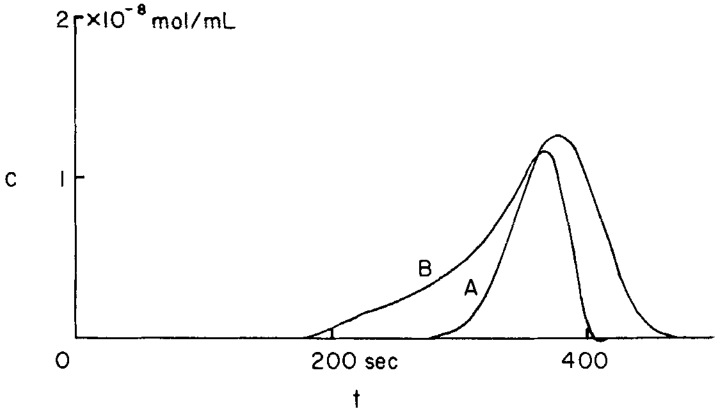

FIG. 10. Effect of concentration-dependent Henry's law constants on band shape. Parameters are from Table 1 except that $K^{ab} = 0$, $K^{ba} = 10^6$ mL/mol.

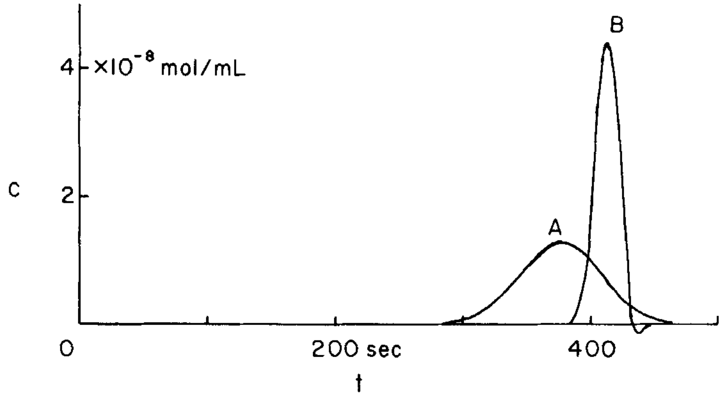

FIG. 11. Effects of concentration-dependent Henry's law constants on band shape. Parameters are from Table 1 except that $K^{ab} = 0$, $K^{ba} = 3 \times 10^6$ mL/mol.

moving down the column, causing B to exhibit a larger retention time than A. This trapping or retardation of B by A has also greatly narrowed the B band, to the point where it is much sharper than the A band which precedes it off the column.

CONCLUSIONS

Numerical integration with advection represented by a linear combination of an asymmetrical upwind algorithm and the theoretical plate algorithm provides a satisfactory technique for modeling solute-solute interactions in preparative gas chromatography. Microcomputers using compiled programs are adequate for these calculations. Solvent-solvent interactions were found to cause changes in retention times, loss of resolution, and severe peak distortion. The effects can be reduced at the cost of reducing sample sizes; computer simulations may be helpful in optimizing this. Changes in retention times and in band shapes may also provide means for studying solute-solute interactions.

Some additional studies which would extend and improve this model are as follows. First, since the stationary phase loadings in preparative columns are generally rather large, one would expect that mass transfer kinetics would be rather important. Earlier we found a time constant approach convenient in handling mass transfer kinetics, and it should be equally satisfactory with these more complex systems. Second, the concentration dependence of the Henry's law constants should be expressed in more detailed and realistic functions than Eqs. (15) and (16).

Acknowledgment

This work was supported by a grant from the National Science Foundation.

REFERENCES

1. K. Tamamushi and D. J. Wilson, *Sep. Sci. Technol.*, *21*, 339 (1986).
2. H. Vink, *J. Chromatogr.*, *20*, 496 (1965).
3. H. Vink, *Ibid.*, *24*, 39 (1966).
4. G. Houghton, *Ibid.*, *15*, 5 (1964).
5. J. C. Giddings, *J. Phys. Chem.*, *68*, 184 (1964) and earlier papers.
6. J. C. Giddings, *J. Chromatogr.*, *2*, 44 (1959).

7. A. Jaulmes, C. Vidal-Madjar, A. Ladurelli, and G. Guiochon, *J. Phys. Chem.*, *88*, 5379 (1984).
8. D. J. Wilson, *Sep. Sci. Technol.*, *21*, 887 (1986).
9. B. P. Leonard, *Comput. Methods Appl. Mech. Eng.*, *19*, 59 (1979).
10. B. P. Leonard, in *Finite Element Methods for Convection Dominated Flows* (T. J. R. Hughes, ed.), American Society of Mechanical Engineers, New York, 1979.
11. K. C. Carter Jr., M. Saenz, D. J. Wilson, and P. W. Rosten Jr., *Environ. Monitor. Assess.*, *4*, 171 (1984).
12. W. Abraham and D. J. Wilson, *Ibid.*, *6*, 145 (1986).
13. D. J. Wilson, *Sep. Sci. Technol.*, *21*, 767 (1986).
14. D. J. Wilson, *Ibid.*, *21*, 991 (1986).
15. A. Ralston and H. S. Wilf, *Mathematical Methods for Digital Computers*, Vol. 1, Wiley, New York, 1965, p. 98.